Application of SQUIDs to phase sensitive experiments (in the $Sr_{1-x}La_xCuO_2$ system)

Victor Leca[1,2,3], Jochen Tomaschko[3], Mihai Danila[1], Di Wang[4], Wim A. Bik[5], Dieter Kölle[3], and Reinhold Kleiner[3]

[1]National Institute for Research and Development in Microtechnologies, Bucharest, Romania
[2]University Politehnica of Bucharest, Faculty of Applied Chemistry and Materials Science, Bucharest, Romania
[3]Center for Collective Quantum Phenomena in LISA+, University of Tübingen, Germany
[4]Karlsruhe Institute for Technology, Institute for Nanotechnology, Karlsruhe, Germany
[5]AccTec BV, TN/Cyclotrongebouw, Technical University of Eindhoven, The Netherlands

Outline

Motivation behind this work

SQUIDs (Superconducting Quantum Interference Devices) – brief description

The $Sr_{1-x}La_xCuO_2$ (SLCO) superconducting compounds and microstructural properties of the SLCO thin films grown by PLD on $BaTiO_3/SrTiO_3$

$Sr_{1-x}La_xCuO_2$ (x=0.145) 30º [001] tilt grain boundary junctions

Symmetry of the superconducting order parameter symmetry for $Sr_{1-x}La_xCuO_2$ (x=0.145) compounds from phase sensitive experiments using 0- and π-dc SQUIDs

Conclusions

Motivation of the work

1. Symmetry of the superconducting order parameter in the electron-doped $Sr_{1-x}La_xCuO_2$ compounds (SLCO, x=0.10-0.175) from:

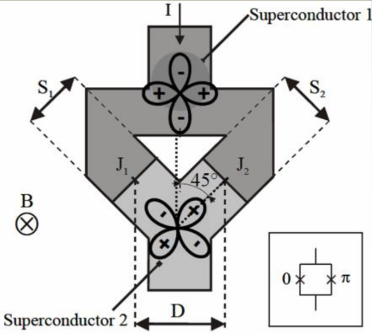

i. tunneling studies across Josephson junctions (grain boundary, ramp-type, planar):

Tomaschko et al., PRB 84, 0214507 (2011)

ii. phase sensitive tunneling experiments based on 0/π-SQUIDs (on $SrTiO_3$ tetracrystals)

Tomaschko et al., PRB 86, 094509 (2012)

2. Studies on SLCO Josephson junctions:

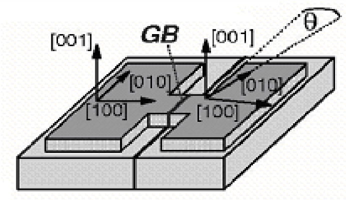

i. grain-boundary junctions based on c-axis oriented SLCO films

Tomaschko et al., PRB 84, 0214507 (2011)

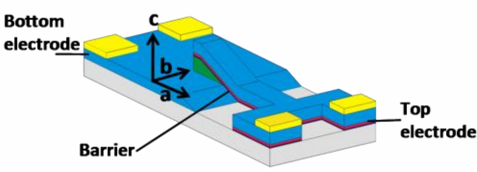

ii. ramp type SLCO/Me/Nb (Me=Ag, Au) junctions

iii. planar c-axis SLCO/Au/Nb tunnel junctions

Tomaschko et al., PRB 84, 064521 (2011)

3. Correlation between strain, microstructure, and electrical transport properties in SLCO thin films grown by PLD on different substrates ($SrTiO_3$, $KTaO_3$, and $DyScO_3$)

Leca et al., APL 89, 92504 (2006); Appl. Phys. A 93, 779 (2008)

Tomaschko et al., PRB 85, 024519 (2012)

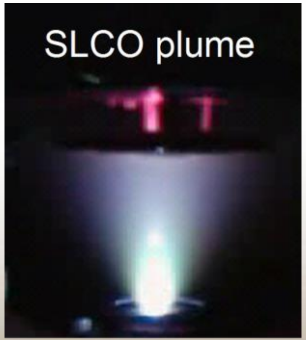

SQUIDs and Josephson junctions– brief description

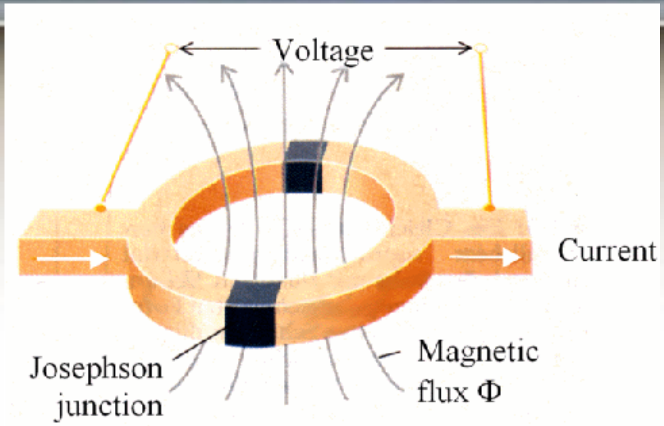

Design of a dc-SQUID

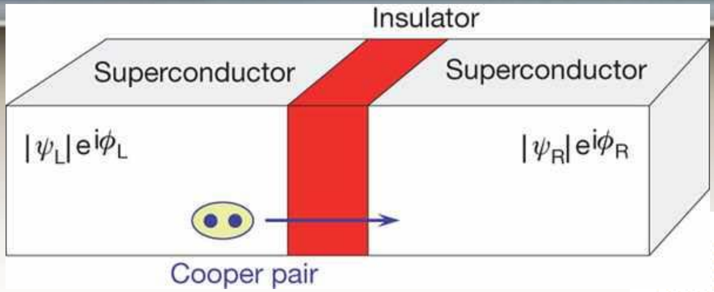

Josephson junction

Grain-boundary Josephson junction

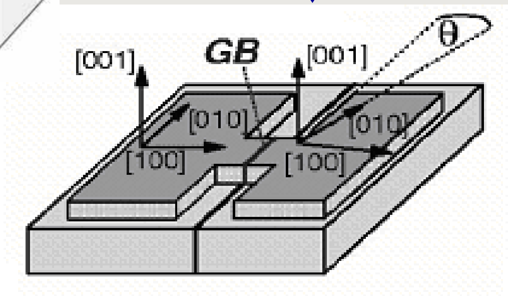

Phase sensitive tunneling:

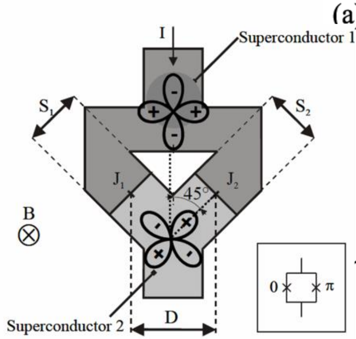

π-phase shift if d-wave symmetry

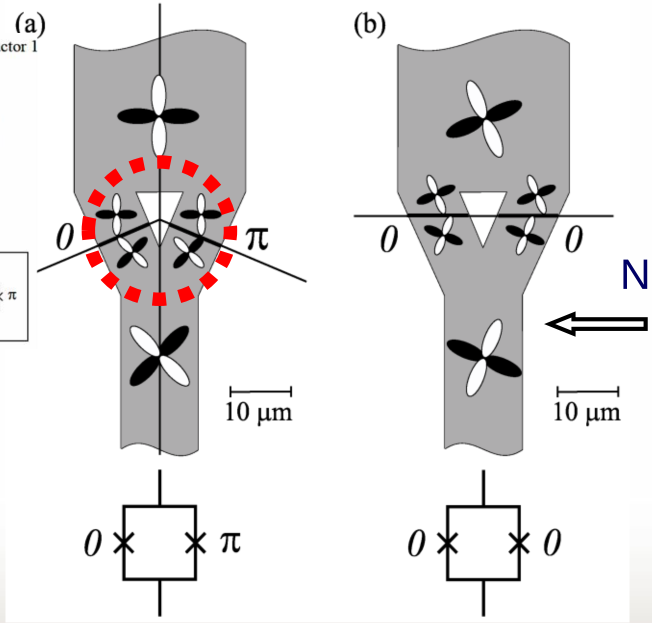

No phase shift

0- and π-SQUIDs

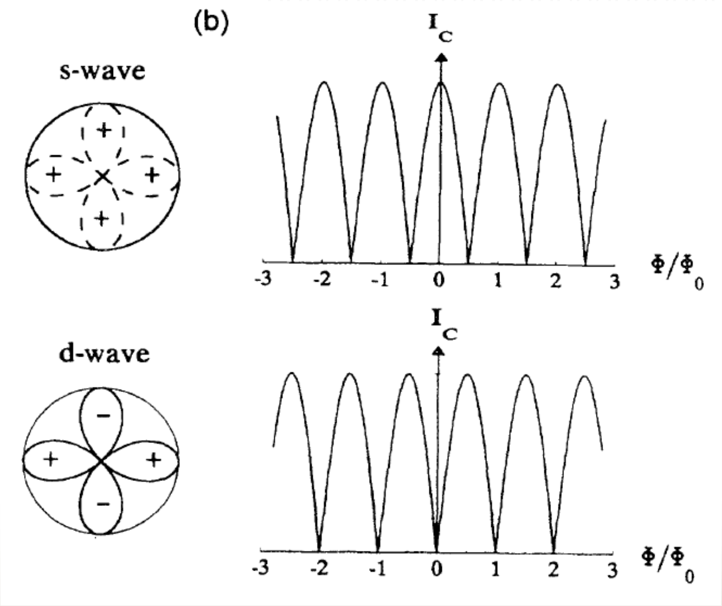

I_c vs applied field for s- and d-wave superconductors

The $Sr_{1-x}La_xCuO_2$ compounds

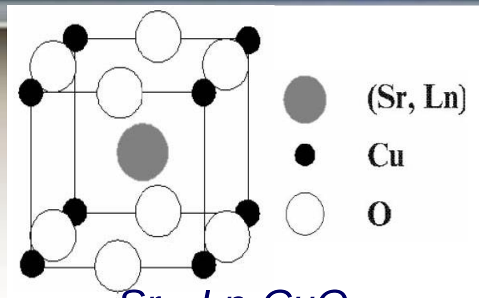

$Sr_{1-x}Ln_xCuO_2$
-infinite-layer (IL) type structure
- $T_{c,max}$ = 43 K

Smith et al., Nature 351 (1991)
Adachi et al., Physica C 196 (1992)

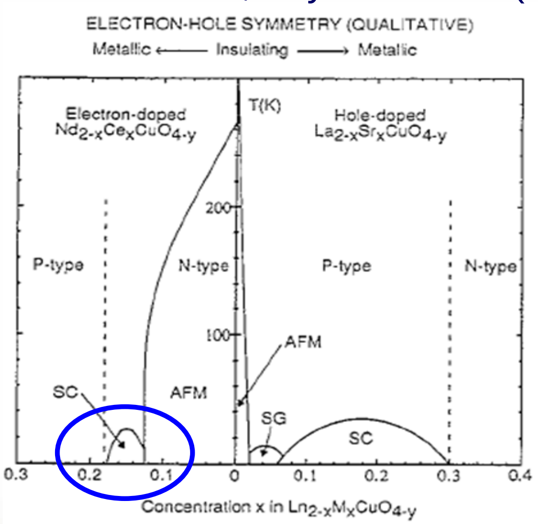

Phase diagram for T'-$Ln_{2-x}Me_xCuO_4$
Armitage et al., RMP 82 (2010)

MBE growth on (001) $KTaO_3$
(reduction method)

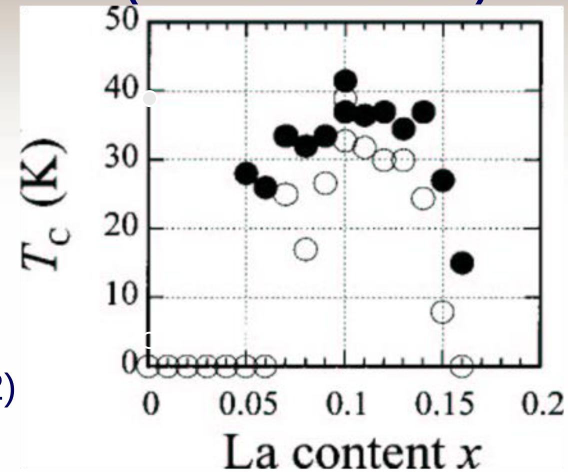

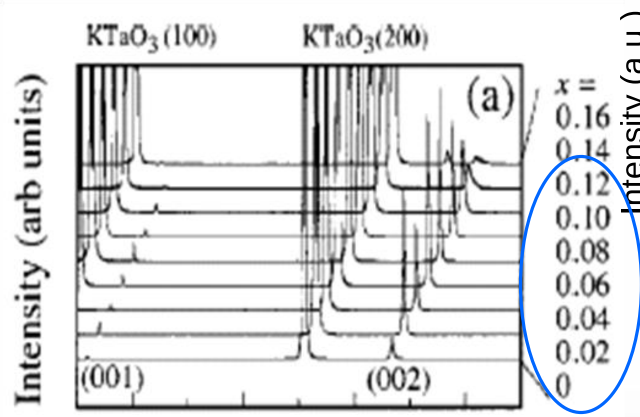

Karimoto et al.
Appl. Phys. Lett. 79 (2001)

PLD growth on (001) $KTaO_3$
(oxidation method)

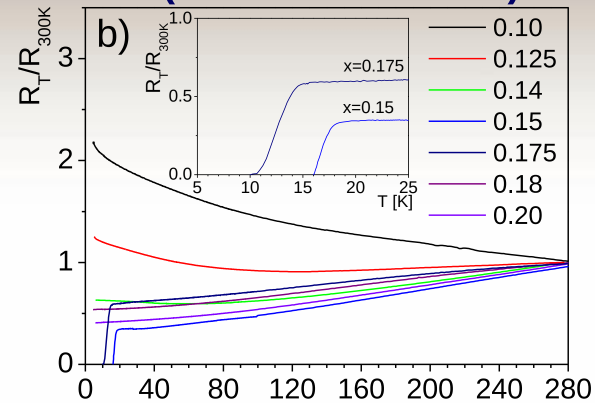

Starting phase:

$2\sqrt{2}a_p \times 2\sqrt{2}a_p \times c$ (super)structure

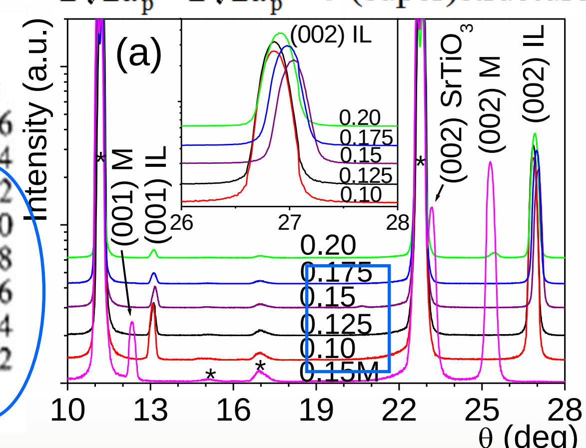

Leca et al.
Appl. Phys. Lett. 89 (2006)

Unknown phase diagram for IL phases

Requirements for GB junctions and films growth parameters

Grain-boundary junctions

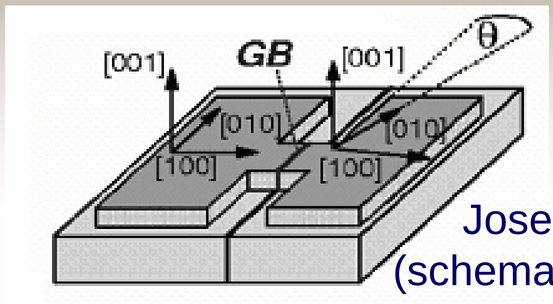

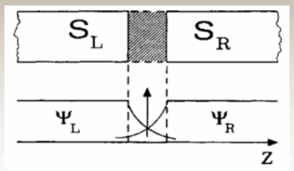

Josephson junction
(schematic representation)

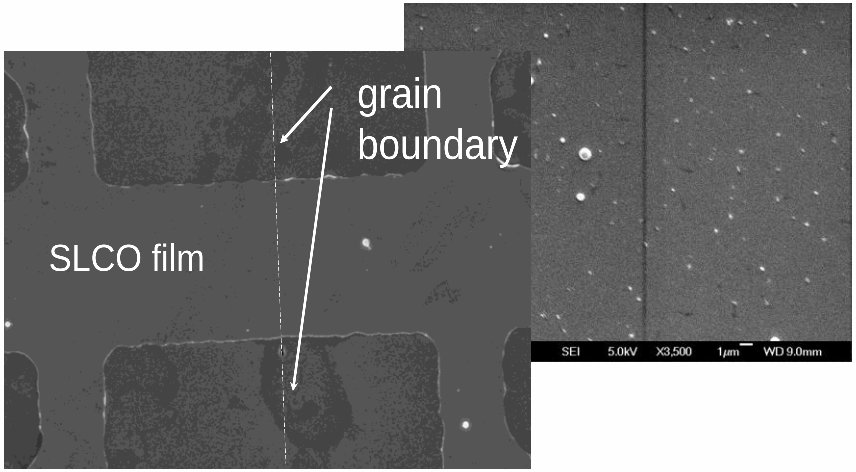

SEM of SLCO grain-boundary junction

Single phase, c-axis oriented films required

On $BaTiO_3$- buffered (001) $SrTiO_3$

$BaTiO_3$ (BTO):

T_d = 700-850 °C
P_d = 0.10 mbar O_2
Post-deposition annealing:
-15 min @ 950°C, under 0.10 mbar O_2, and
30 min @ 950°C, in vacuum (10^{-7} mbar)

$Sr_{1-x}La_xCuO_2$ (SLCO):

T_d = 550-600 °C
P_d = 0.20 mbar O_2
Post-deposition annealing (reduction):
45-60 min @ 550 °C, in vacuum (10^{-7} mbar)

T_c: up to 21 K

Film's composition (x_t = 0.15 target),
from RBS data: x_f = 0.145

a_{STO}=3.905 Å, a_{BTO}~3.987 Å, a_{SLCO}~3.967 Å

$Sr_{1-x}La_xCuO_2$ ($x \approx 0.15$) grown on $BaTiO_3/SrTiO_3$ (001)

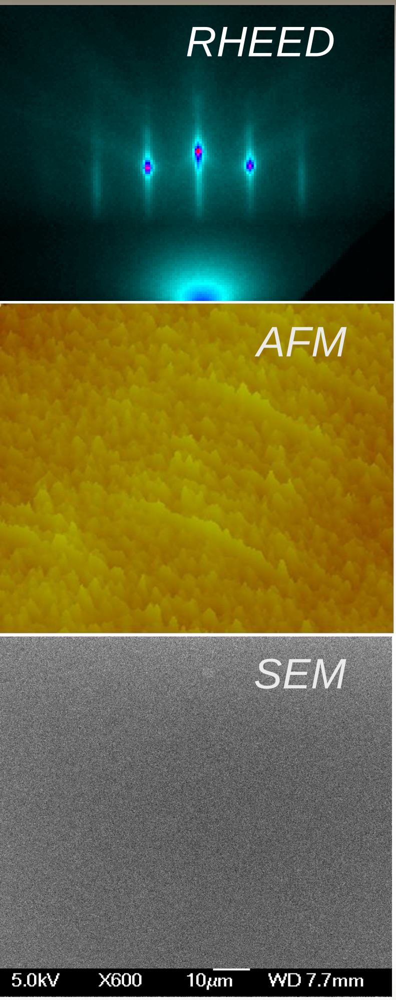

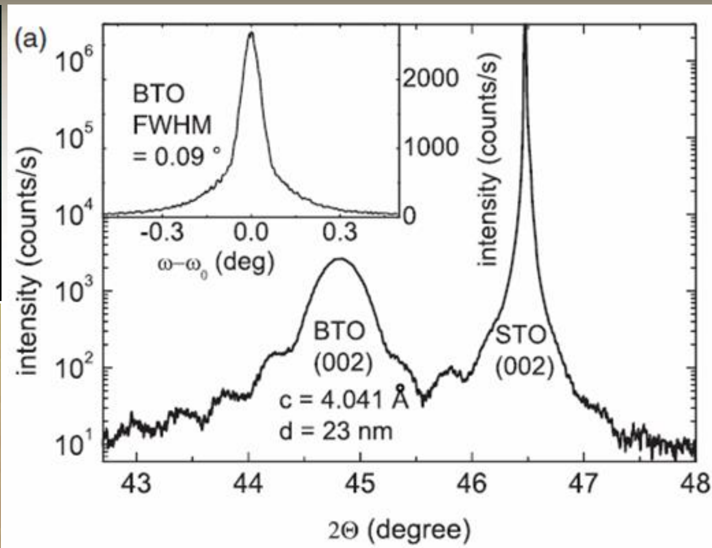

XRD 2θ/ω and rocking curve scans of BTO/STO symmetric (002) reflection; film thickness estimated from Laue fringes

The $BaTiO_3$ buffer layer

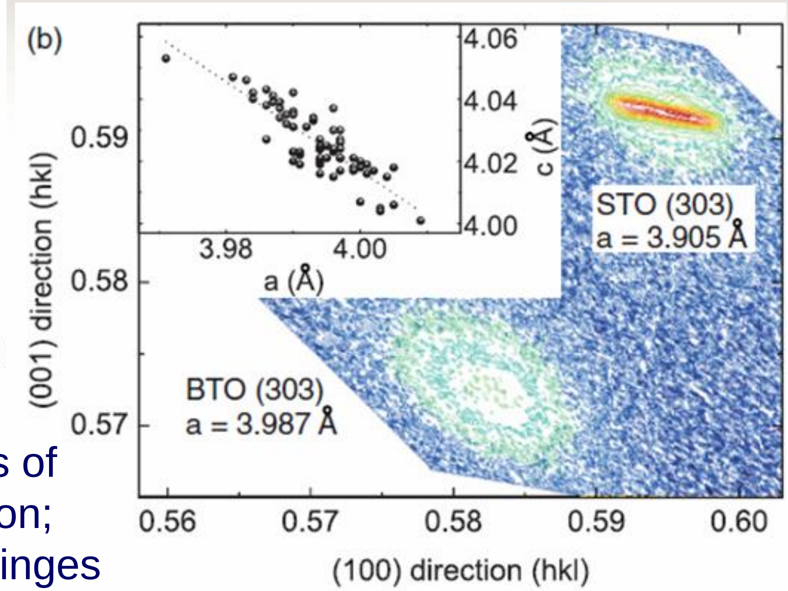

XRD rsm around asymmetric (303) Bragg reflection of BTO/STO

Tetragonal symmetry

Deposition conditions for $BaTiO_3$:

T_d=750°C, P_d=0.10 mbar O_2, E_d=1.75 J/cm^2;

annealing 15 min/950°C/0.10 mbar O_2 and 30 min/950°C/10^{-7} mbar

Tomaschko et al., Phys. Rev. B 85 (2012)

$Sr_{1-x}La_xCuO_2$ ($x \approx 0.15$) grown on $BaTiO_3/SrTiO_3$ (001)

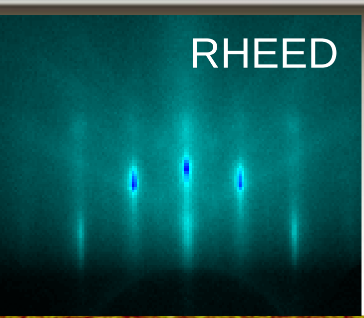

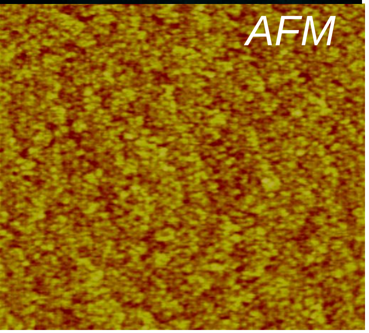

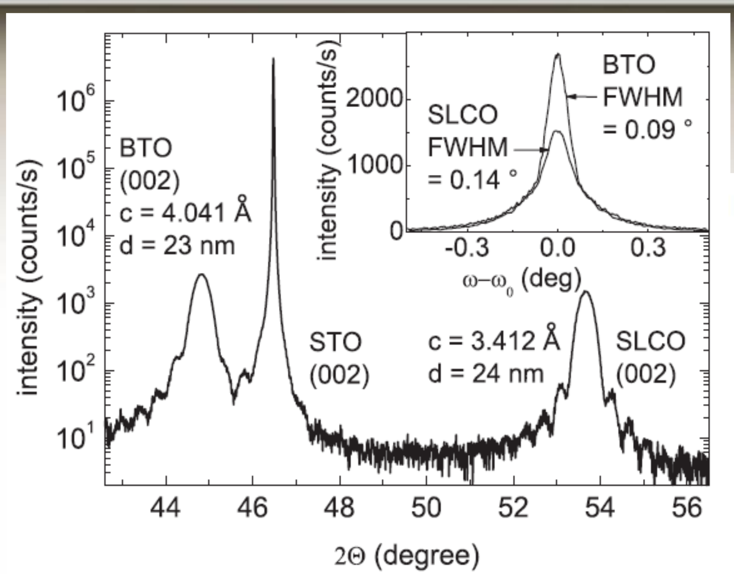

XRD 2θ/ω and rocking curve scans of (002) reflections

The $Sr_{1-x}La_xCuO_2$ films

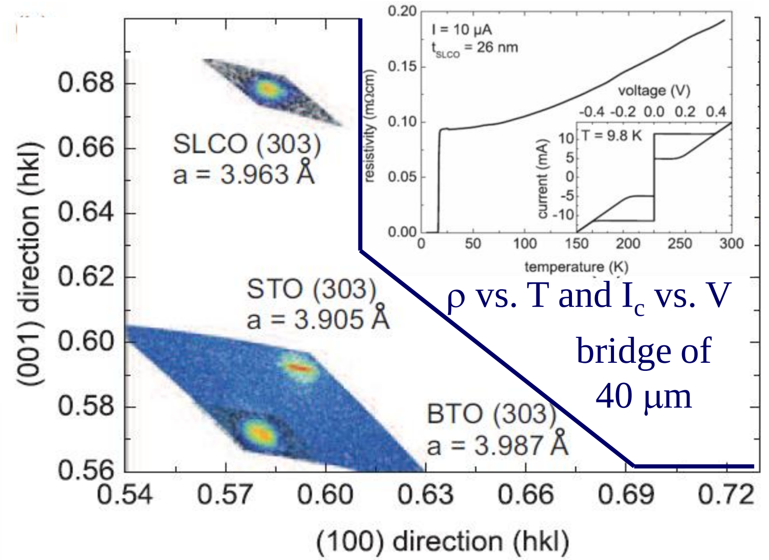

XRD rsm of (303) SLCO/BTO/STO

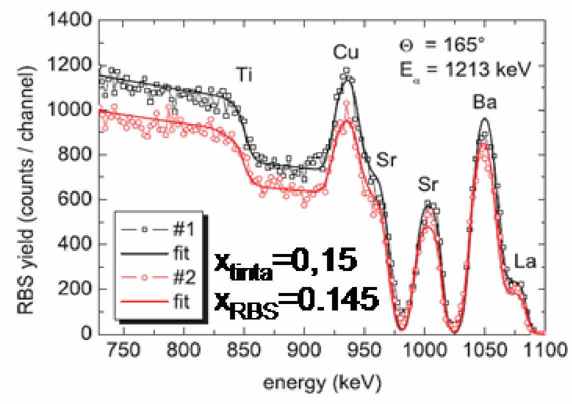

RBS data

No presence of secondary phase; tetragonal,
IL-type structure; preferential orientation (c-axis)

Deposition conditions for $Sr_{1-x}La_xCuO_2$:

T_d=550°C, 0.30 mbar O_2; annealing 50 min/550°C/10^{-7} mbar

$T_{c,0}$=≤ 21 K; $J_{c@4.2K}$ =2.1×10^6 A/cm^2

Tomaschko et al., Phys. Rev. B 85 (2012)

$Sr_{1-x}La_xCuO_2$ ($x \approx 0.15$) grown on $BaTiO_3/SrTiO_3$ (001)

Microstructure

HRXRD

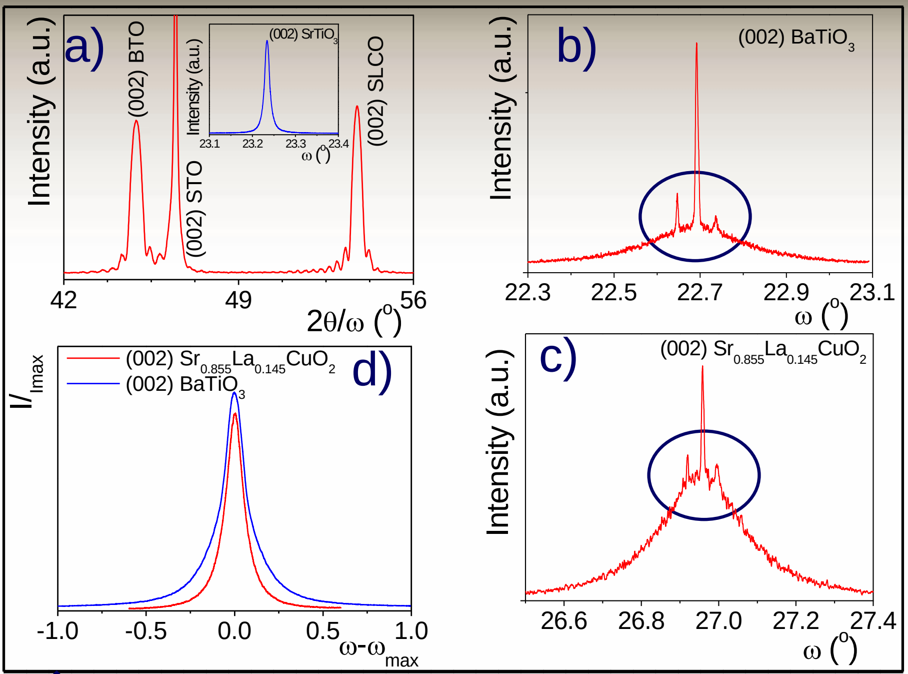

HRXRD (a-c) and XRD (d) data for a BTO/SLCO film with d_{BTO}=35 nm

Misfit strain accommodation by lattice modulations

Two components in ω scans: strained and relaxed

Buffer layer thickness dependent microstructure:
- lattice modulations visible ***only*** in the HRXRD scans and for d_{BTO} > 30 nm

HRXRD: triple axes configuration
XRD: double axes configuration

HRSTEM

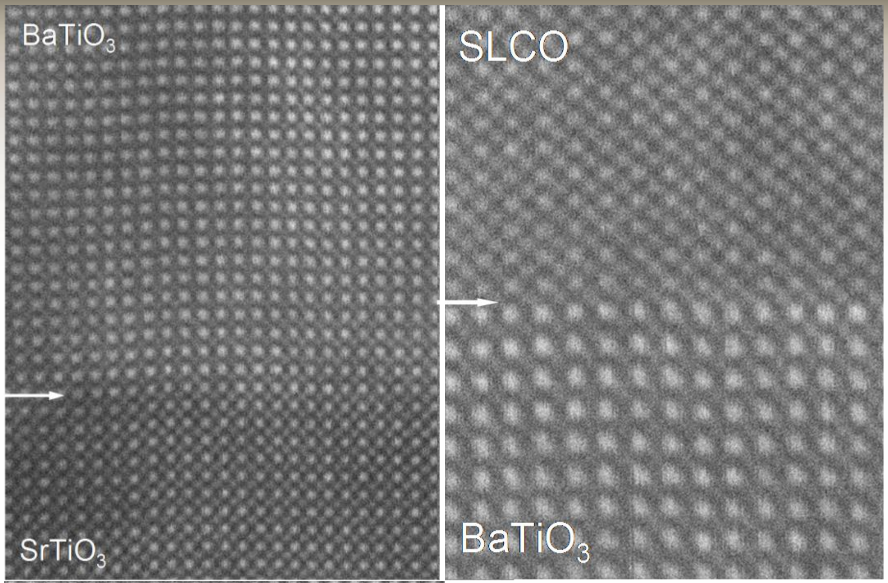

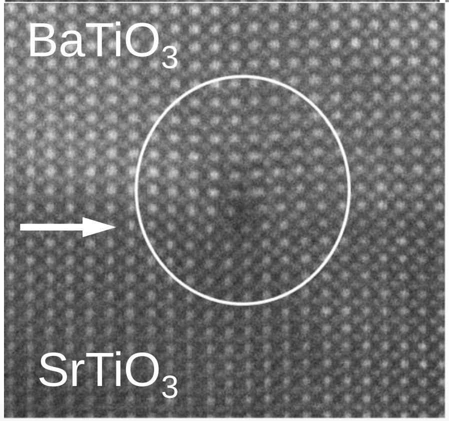

edge dislocation at the STO/BTO interface

Migration of the structural defects at the BTO/STO interface due to high temperature annealing

Terai et al., APL 80 (2002)

$Sr_{1-x}La_xCuO_2$ 30º symmetric grain boundary junctions

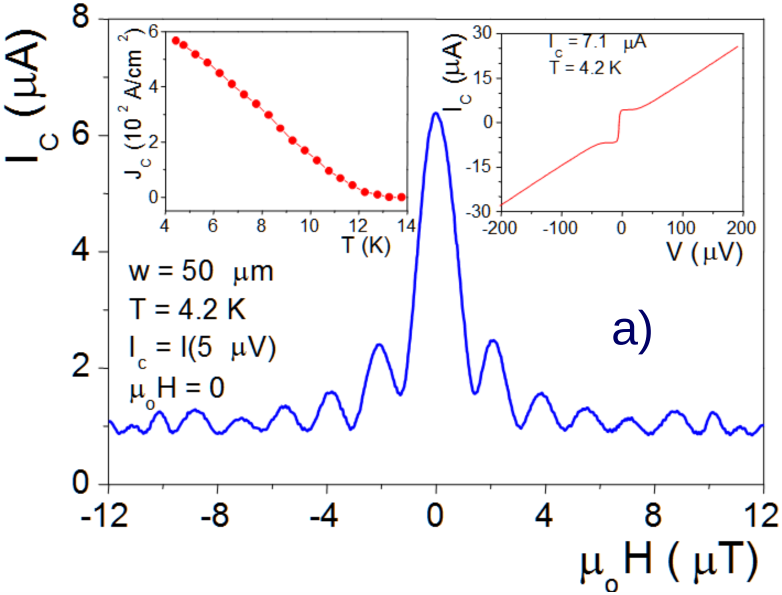

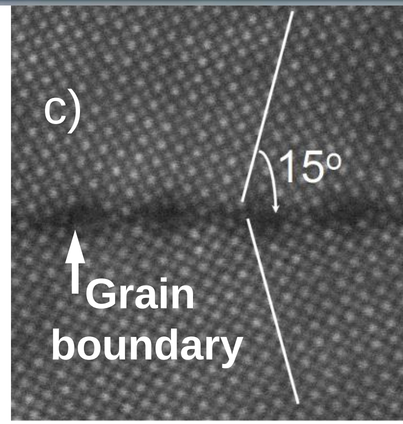

HRSTEM image ($SrTiO_3$ bicrystal)

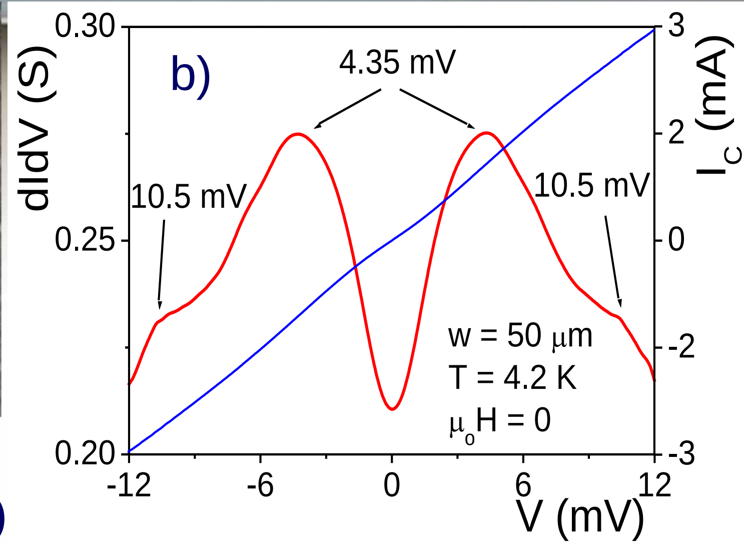

Conductance spectra

I_CH, J_cT, and I_cV characteristics

a) I_cVs: resistively and capacitively shunted junction (RCSJ)-like;
- highly regular Fraunhofer-like patterns;
- high J_c @ 4.2 K of ~ 0.55 kA/cm^2; I_cR_n of ~ 50 μV

b) conductance spectra did not show a zero-bias conductance peak-ZBCP (but a V-shaped subgap spectra) ***and*** extra peaks above the coherence peaks; microscopic roughness?
- possible first observation of the two band structure (due to holes and electrons charge carriers);

c) plain view HRTEM of the substrate (30º) grain boundary.

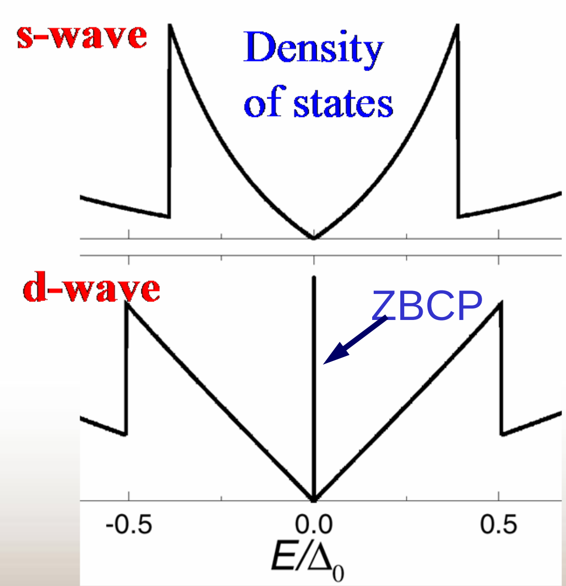

Pairing symmetry from phase sensitive experiments

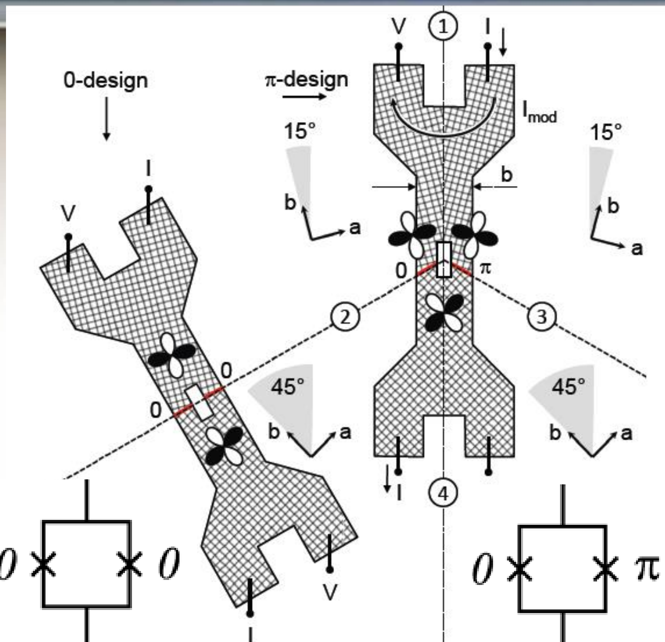

Schematic layout of the 0 - and π-SQUIDs

[Schulz et al., APL 76 (2000); Chesca et al., PRL 90 (2003)]

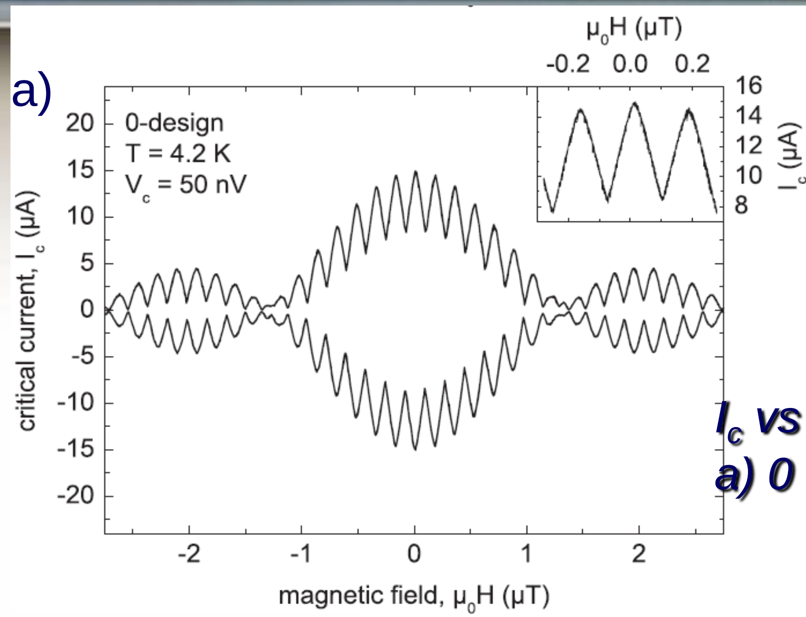

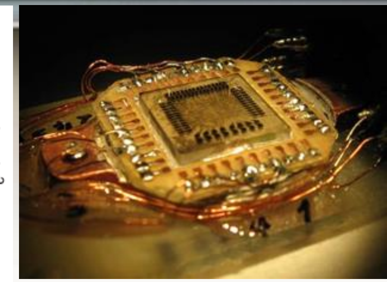

I_c vs magnetic field for a) 0 - and b) π-SQUID

Geometry designed to be frustrated for d-wave pairing;
If d-wave: the dc-SQUID ring around the tetracrystal point contains one 0-junction and one π-junction (forming the π-SQUID, which exhibits an additional π shift in its phase).

The I_c vs. H shows a minimum at H=0 for the π-SQUID due to the phase shift across the π-junction.

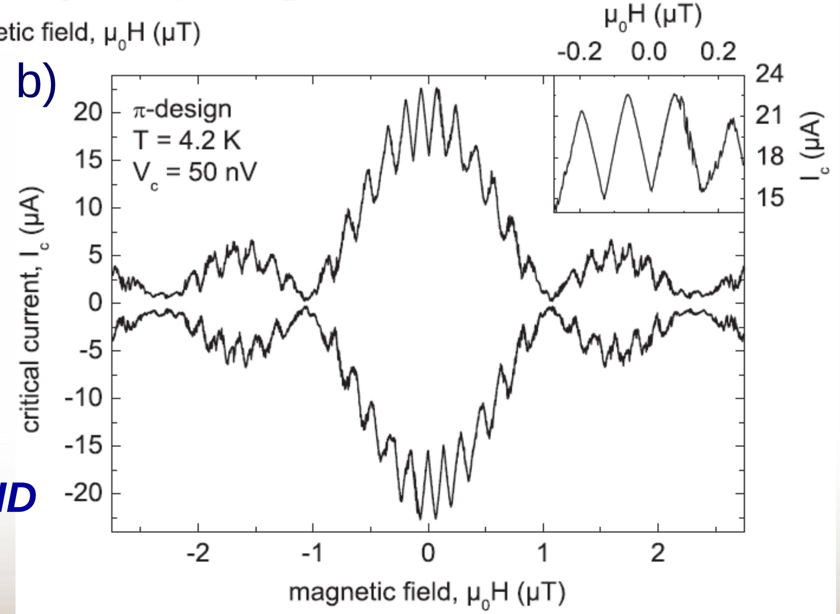

Predominantly $d_{x^2-y^2}$ pairing symmetry

Tomaschko et al., Phys. Rev. B 86 (2012)

Conclusions

- no zero bias conductance peak observed in grain-boundary junctions, most probably due to oxygen vacancies along the grain boundary;

- phase sensitive experiments shown a predominantly d-wave order parameter symmetry in the $Sr_{0.855}La_{0.145}CuO_2$ thin films;

- the superconducting properties of the PLD grown electron-doped $Sr_{1-x}La_xCuO_2$ thin films are still far of those of the bulk or of the MBE grown films; however, higher phase stability can be achieved by PLD (in the over doped region).

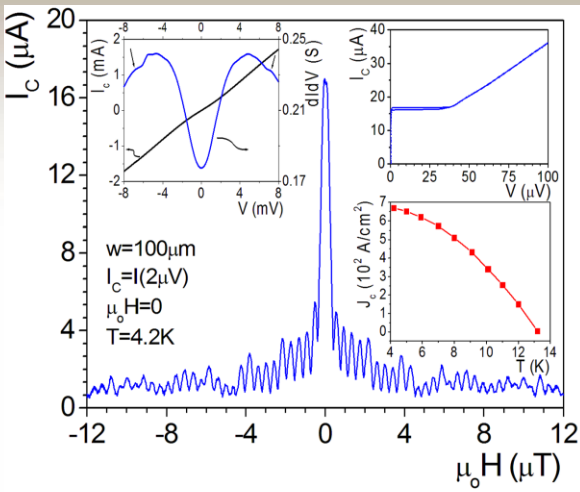

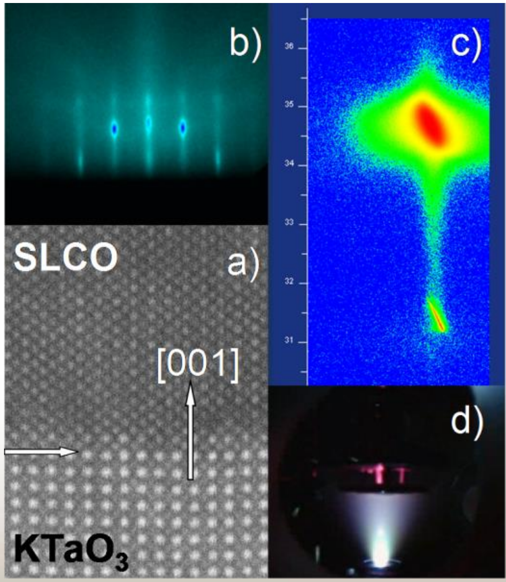

Acknowledgements

Deutsche Forschungsgemeinschaft (project KL 930/11)

Romanian National Authority for Scientific Research, CNCS UEFISCDI, project number PNII-ID-PCE-2011-3-1065

European Commission under the FP7 Capacities programme (EUMINAfab project number 1090)